International Journal of Engineering & Technology, 7 (4.26) (2018) 153-158

International Journal of Engineering & Technology

Website: www.sciencepubco.com/index.php/IJET

Research paper

Theoretical Bending Collapse of Hat-Section Tubes

Hafizan Hashim[1]*, Hanita Hashim [2], Arif Affendi Jamal [3], M.A.M. Jusoh[4]

[1]Faculty of Mechanical Engineering, Universiti Teknologi MARA (UiTM), 40450 Shah Alam, Selangor, Malaysia
[2]Faculty of Engineering and Life Sciences, Science and Biotechnology Cluster, Universiti Selangor (UNISEL), Jln Timur Tambahan, 45600 Bestari Jaya, Selangor, Malaysia
[3]Insitute of Product Design & Manufacturing, Universiti Kuala Lumpur (UniKL), 56100 Cheras, Kuala Lumpur, Malaysia
**Corresponding author E-mail: hafizandes@gmail.com*

Abstract

This paper presents an attempt to modify an existing theoretical model to predict the bending collapse response of hat-section tubular structures. The analytical collapse model was based on Kim and Reid. Additional hinge lines created during deformation of the tube were examined and integrated with existing model to forming a modified analytical solution. Variation of the hinge moments were solved using limit analysis technique. Procedure for developing the finite element (FE) models of tube specimens was also presented. Moment-rotation characteristics from pure bending simulation were compared with analytical model and good agreement was achieved. The average of differences between simulation and calculation were found to be <5% within plastic region. In conclusion, the modified analytical solution has adequate capability to predict the moment-rotation relationship of hat-section tubes subject to pure bending.

.

Keywords: *Bending; Hat-section; Hinge mechanism;Finite element.*

1. Introduction

Thin-walled structure is a kind of typical energy absorbers used in many applications such as automotive, naval, and aerospace. Over the past decades, many efforts have been made to improve their crashworthiness, however axial progressive collapse succeeded only in laboratory and fails in the real crash. Under external impact load, a thin-walled beam tends to bend due to instability and minimal energy absorption. Real crash scenario shows that almost 90% of structural members involved in an accident failed in bending collapse mode [1]. Therefore, study on the bending behaviour of thin-walled energy absorbers is essential for their improvement. Among vehicular structural members is a generic form of steel profiles known as hat-section tube. They are used due to their excellent light weight to protect occupant and other assets against impact loads. During impact, bending deformation is a basic deformation exhibited by hat-section tube. It becomes a theoretical basis for body structure design that is studied under bending collapse theory.

The study of bending behaviour of thin-walled tubular structures was first reported by Abramowicz and Wierzbicki [2] and Kecman [3]. Both approaches involved nonlinear geometrical problems in plasticity. The mathematical equations derived by Kecman [3] relate hinge moment and rotation angle during post collapse that involve stationary and moving plastic hinge lines. The bending moment of the whole sections showed a good agreement between theoretical predictions and experiment results. Wierzbicki et al. [4] proposed a collapse model based on the moving hinge lines within a small angle range. This model was further improved by Kim and Reid [5] by introducing a new kinematically admissible folding mechanism to predict bending collapse of square and rectangular cross section tubes. It closely resembles Kecman's model [3] with inclusion of some in-plane deformation and introduced two additional free parameters from total plastic work.

Compared with typical thin-walled tubes, the hat-section tubes with the same parameter possess higher flexibility in terms of manufacturability and workability. Related studies showed that the hat-section tubes are versatile and reflect the actual application in real world with higher hybrid ability [6-10]. Nevertheless, study on the collapse behaviour and analytical approach to estimate moment-rotation relationship has received less attention [11]. This paper re-examines the bending collapse mechanism of hat-section tubes and suggests an analytical solution to determine the moment-rotation relationship. The collapse model is based on Kim and Reid [5] which is originated from Kecman [3] and Weizbicki et al. [4] by addressing some issues found in both previous models. This work includes development of finite element (FE) model using an explicit non-linear FE programme, ABAQUS. The validated model was used to simulate pure bending in order to verify the modified analytical results. Comparison results show good agreement and the modified analytical approach is therefore validated.

2. Bending Collapse Mechanism: Kim and Reid's Approach

For applying this analytical approach, an idealized collapse mechanism for present collapse modal is considered. Fig. 1 shows a theoretical collapse model of a hat-section tube subject to pure bending. During the hinge development, there are about four phases describe the actual bending collapse mechanism of a hat-section tube. The first phase occurs by a protruding bulge in the webs at a fixed location without rolling deformations. It follows by the second phase when the bulge starts to roll along yield lines GA, AK, and their symmetric counterparts. In the next phase, the rolling deformation due to the moving bulge was put to the end when jamming mechanism initiated from the creation of the secondary hinge and the hinge continues to develop in the final phase

of the collapse mechanism. Fig. 1 shows detail geometry of the tube folding mechanism. It looks quite similar to Kecman's model, with inclusion of some in-plane stretching to enable the folding process to be determined kinematically. According to upper bound solution of minimum total plastic work, two new parameters which are *H* and *r* are to be determined. Due to mirror symmetry, the following calculation considers only the half section of the tube.

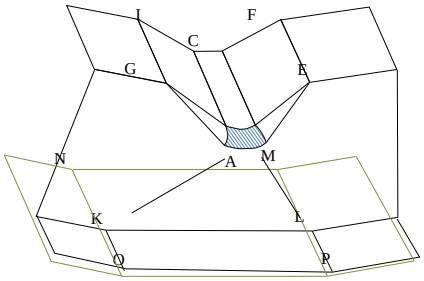

Fig. 1: A new folding mechanism of hat-section beam (half the section).

2.1. Calculation of Energy Absorbed

2.1.1. Kinematics Analysis of the Collapse Model

This theoretical approach is based on the work of Kim and Reid [5] with few modifications on the additional sections which are the lips and closed-plate. The kinematics of the H0 beam collapse model is defined with reference to Fig. 2. The beam is subjected to pure bending and the folding mechanism take place at a specified position on a portion of it surface. The folding mechanism is considered kinematically admissible when some of the displacement or velocity distribution in the folding segments is specified on other portions of the beam are continuous and satisfies the velocity and displacement boundary condition. Dimension of the flange width, $W_f = b_f = a\text{-}t$ and web width, $W_w = b_w = b\text{-}t$ are defined from the center of the plate (i.e. mid-plane). Here, *a* and *b* are the approximate outer dimension (nominal dimension) for the beam section and *t* is the shell thickness. In Kecman's model [3], the control parameter α is produced from relative rotation of flange wall along GH and it is measured from deformed GB to deformed flange plane. In Kim and Reid [5], the α is defined differently when it is measured from the original flange's plane.

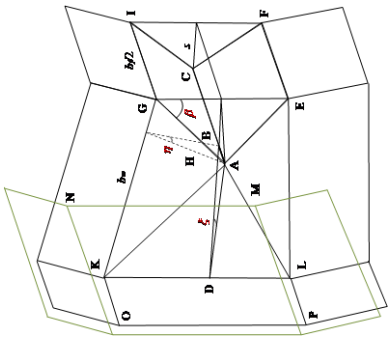

Fig. 2: Hinge section, half model geometry of a hat-section tube

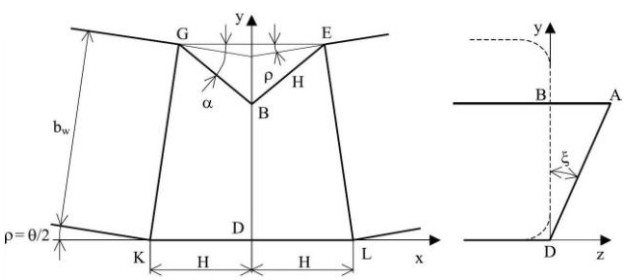

Fig. 3: Longitudinal section of the bending mechanism of hat-section tube.

The angle ρ is defined similarly by these two models, $\rho = \theta/2$ with θ denotes the angle of hinge rotation. We can relate α and ρ as:

$$\alpha = \frac{\pi}{2} - \arcsin\left(1 - \frac{W_w}{H}\sin\rho\right) \tag{1.1}$$

The coordinates of the point B in Fig. 2 are:

$$x_B = 0 \quad , \quad y_B = W_w \cos\rho - H \sin\alpha \tag{1.2}$$

Assuming the bulge in the mid-section expands continuously and from continuity condition, point A becomes:

$$y_A = y_B = W_w \cos\rho - H \sin\alpha \tag{1.3}$$

$$\frac{(W_w)^2 - (y_B)^2}{2W_w} = z_A \tag{1.4}$$

Point C in the mid-section displaces by *s* down vertically at the rate of, *v*, thus:

$$s = H \sin\alpha + W_w(1 - \cos\rho) \tag{1.5}$$

$$v = \dot{s} = H\cos\alpha\,\dot{\alpha} + W_w \sin\rho\,\dot{\rho} \tag{1.6}$$

Considering half of the toroidal section in Fig. 2(a), the angle β of relative rotation of diagonal line GA about original flange edge becomes:

$$\beta = \arccos\left(\frac{H\cos\alpha}{\sqrt{(H)^2 + (z_A)^2}}\right) \tag{1.7}$$

2.1.1. Classification of Hinge Lines

As shown in Fig. 2 and 3, the hinge lines for an ideal half H0 beam model is comprised of compressed flanges (GACI and EACF), tensile flanges (MNOP), tensile lips (OK and PL), and a protruded web (EGKL). Plastic deformation is assumed to occur merely along hinge lines within generalized beam hinge of 2H. The hinge lines where plastic energy is dispelled can be classified as tabulated in Table 1.

Table 1: Classification of hinge lines

No	Hinge lines	
	Class of hinge lines	Location
1	**Stationary hinge lines**	
1.1	Compression flange	GI, EF, AC
1.2	Web	GK, EL, KL
1.3	Tensile flange (closed-plate)	ON, PM
1.4	Tensile lips	OK, PL
2	**Rolling hinge lines**	
2.1	Edge	AG, AE
2.2	Web	AK, AL
3	**Continous velocity field**	
3.1	Toroidal surface	A (Refer Fig. 1)

3. Plastic Energy Dissipation and Moment-Carrying Capacity of Plastic Hinges

3.1. Rate of Plastic Energy Dissipation

Continuous and discontinuous velocity fields have resulted in energy dissipation from folding process of rigid and perfectly plastic shells as stated in:

$$\dot{E} = \int_s \left(M_{\alpha\beta}\dot{\kappa}_{\alpha\beta} + N_{\alpha\beta}\dot{\varepsilon}_{\alpha\beta}\right) \mathrm{d}S + \int_l M_0\,\dot{\theta}\,\mathrm{d}l \tag{1.8}$$

where $\dot{\kappa}_{\alpha\beta}$ and $\dot{\varepsilon}_{\alpha\beta}$ are curvature and extension rates respectively. The $N_{\rho\beta}$ and $M_{\rho\beta}$ are membrane forces and bending moments respectively. All that contains in the left hand side of (1.8) are defined from the Cauchy stress tensor. In the second part of opposite side, the fully plastic bending moment is given by $M_0 = \sigma_0 (t^2/4)$. During the deformation progress, both extensions from continuous plastic deformation S and the hinge line l increase. The θ denotes finite rotation around every hinge line. The dissipated energy is calculated in the first integral of (1.8) for which the extensional deformation of the toroidal surface is considered as shown in Fig. 3. On the other hand, the second integral calculates the dissipated energy of bending around the hinge lines. In every hinge line, membrane-bending interaction is neglected, only the rates of energy dissipation are calculated.

3.2. Energy Dissipation in a Sheet Passing Over a Toroidal Surface

For the toroidal segment shown in Fig. 3, a generic point within this surface may be described by two coordinates (θ,ϕ). Here, θ denotes the meridian coordinate and is along the circumferential direction as shown in Fig. 3(b) and (c) respectively. The limits of θ and ϕ are:

$$\frac{\pi}{2} - \psi \le \theta \le \frac{\pi}{2} + \psi \tag{1.9}$$

$$-\beta \le \phi \le \beta \tag{1.10}$$

Also:

$$R = r\cos\theta + a \tag{1.11}$$

where r is the radius in the meridian direction. When a material is forced to pass outward over this toroidal surface, there is a circumferential strain and its increment corresponding to a tangential velocity v_t is:

$$\dot{\varepsilon}_{\phi} = \frac{v_t \sin\theta}{R} = \frac{H\cos\alpha\,\dot{\alpha}}{\tan\psi_0}\frac{\sin\theta}{r\cos\theta + a} \tag{1.12}$$

Here, $v_t \sin\theta$ is the horizontal component of v_t, and:

$$v_t = \frac{\dot{s}}{\tan\psi_0} = \frac{H\cos\alpha\,\dot{\alpha}}{\tan\psi_0} \tag{1.13}$$

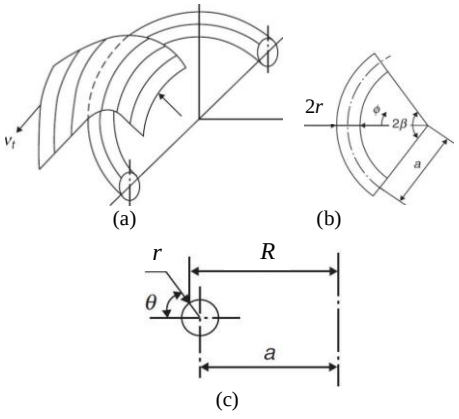

Fig. 3: Example of an image with acceptable resolution

In the toroidal region, the main plastic flow occurs in terms of $\dot{\varepsilon}_{\phi}$. Though there is a non-zero curvature change in circumferential direction, the corresponding bending energy can be shown to be zero (resulting from the fact that yielding occurs in circumferential tension with a fully yielding membrane force $N_0 = Yh$). Since, there is only two non-vanishing components of the generalized strain rate tensor, the yield condition becomes $\left|\frac{M_{\phi\phi}}{M_0}\right| + \left(\frac{N_{\phi\phi}}{N_0}\right)^2 = 1$. For $R/r > 2$, the membrane forces become $N_{\phi\phi} = N_0$, subsequently reducing $M_{\phi\phi} = 0$. Hence, the plastic dissipation rate is:

$$\dot{E}_{\text{tor}} = \int_s N_0\dot{\varepsilon}_{\phi\phi}\,\mathrm{d} = 16\frac{M_0 r}{t}(H\cos\alpha\,\dot{\alpha} + W_w \sin\rho\,\dot{\rho}) * \int_0^{\beta(H,\rho)} \frac{1}{\sqrt{1+\cos^2\phi}}\mathrm{d}\phi \tag{1.14}$$

where dS is the surface element. Equation (1.14) has been derived in details by Wierzbicki et al. and Abramowicz and Wierzbicki. In the case of the axial compression, the velocity of point C in the horizontal direction increases by H sin $\alpha\dot{\alpha}$, but for bending kinematics, the vertical velocity is defined by W_w sin $\rho\dot{\rho}$. When the bending is initiated, H vary with toroidal portion, β, or β becoming a function of H and the angle of rotation.

3.3. Energy Dissipation in a Sheet Passing Over a Toroidal Surface

The rolling hinge lines in conical shape AG and AE have two edges of straight lines and the curve of a circle of radius r. Refer to (1.6), the rate of rotation in meridian direction along the hinge line should be constant and equal to $\dot{\theta} = v / r$. Length GA is assumed to has approximate length with hinge lines, L, thus the dissipated energy becomes:

$$\dot{E}_{\text{GA+EA}} = \sum_i M_0\, l_i\dot{\theta}_i = 4M_0\sqrt{(H)^2 + (z_A)^2}\frac{H\cos\alpha\,\dot{\alpha} + b_w \sin\rho\,\dot{\rho}}{r} \tag{1.15}$$

where the discontinuity of rotation rate in the meridional direction, $\dot{\theta}$, is assumed constant along GA as well as the toroidal region.

3.4. Energy Dissipation in Web through the Rolling of Hinge Lines

The equation suggested by Kecman [3] and Mahmood et al. [12] was used to estimate the amount of absorbed energy in the web through the rolling of hinge lines:

$$W_r = 2\,M_0\int_0^{KA}\frac{l_r(L)}{r_r(L)}\,\mathrm{d}L \tag{1.16}$$

where l_r (L) represents the rolling distance and r_r (L) is the radius of travelling hinge, which may have linear variation along L. Following assumption is made as in Kecman , therefore the total energy absorbed along KA becomes:

$$W_{KA} = \frac{2}{3}\frac{M_0}{r}\text{KA}z_A \tag{1.17}$$

the distance KA $= \sqrt{(H)^2 + (z_A)^2 + (y_B)^2}$. By differentiating (1.17) with respect to time plus applying mechanism KA to LA, the total dissipated energy along KA and LA is given by:

$$\dot{E}_{\text{KA+LA}} = \frac{4}{3}\frac{M_0}{r}\frac{\mathrm{d}}{\mathrm{d}t}(\text{KA}z_A) \tag{1.18}$$

3.5. Stationary Plastic Hinge Lines

There are five stationary plastic hinges which subject to compression and tensile that absorbed plastic energy in the flange and web. Except AC, the rest of hinge lines are assumed to have constant length during folding process and calculated as below.

(i) Compressed flange

$$\dot{E}_{\mathrm{EF+GI}} = \sum_i M_0\, l_i \dot{\theta}_i = M_0 W_f(\dot{\alpha} - \dot{\rho}) \tag{1.19}$$

$$\dot{E}_{\mathrm{AC}} = \sum_i M_0\, l_i \dot{\theta}_i = 2M_0 \left(\frac{W_f}{2} + z_{\mathrm{A}}\right)\dot{\alpha} \tag{1.20}$$

(ii) Web

$$\dot{E}_{\mathrm{GK+EL}} = \sum_i M_0\, l_i \dot{\theta}_i = 2M_0 W_w \dot{\eta} \tag{1.21}$$

where $\eta = \arcsin\left(\frac{z_A}{H}\right)$.

$$\dot{E}_{\mathrm{KL}} = \sum_i M_0\, l_i \dot{\theta}_i = 2M_0 H \dot{\xi} \tag{1.22}$$

where $\xi = \arctan\left(\frac{z_A}{y_B}\right)$.

(iii) Tensile flange (closed-plate)

$$\dot{E}_{\mathrm{KN+LM}} = \sum_i M_0\, l_i \dot{\theta}_i = M_0 W_f \dot{\rho} \tag{1.23}$$

(iv) Tensile lip

$$\dot{E}_{\mathrm{OK+PL}} = \sum_i M_0\, l_i \dot{\theta}_i = M_0 W_l \dot{\rho} \tag{1.24}$$

4. Approximate Instantaneous Moment

The approximate instantaneous moment applied on the folding section can be defined by the three unknowns (i.e. $H, r, \theta,$ or ρ). Applying the principle of virtual work:

$$\dot{E}_{\mathrm{ext}} = \sum \dot{E}_{\mathrm{int}}, \; M = M(H, r, \theta) \tag{1.25}$$

The instantaneous moment $M(\theta)$ is a function of H and r which are the plastic folding length and the rolling radius respectively. The folding process leads to the least possible amount of the instantaneous folding force. Therefore, the limitation of the mean value should be considered as described by Wierzbicki and Abramowicz [2]. Integrating (1.25) up to the total folding angle gives equivalent mean crushing moment.

$$M_m(H, r) = \frac{1}{\rho_{\mathrm{f}}(H)} \int_0^{\rho_{\mathrm{f}}(H)} M \, \mathrm{d}\rho \tag{1.26}$$

where $\rho_{\mathrm{f}}(H)$ is the jamming angle.
Based on Fig. 2, the idealized collapse model of H0 beam produces the theoretical jamming angle of arc sin (H/b_w). Kecman [3] suggested that the jamming angle should be $\arcsin\left\{\frac{(H-0.5t)}{b_w}\right\}$ when the wall thickness is considered. Based on experimental observation, this relationship valid for shallow rectangular sections with $a > b$. For section with $b > a$, it was reported that the shell thickness and deformed web affects the hinge when the jamming occurs earlier. The information on this however is not conclusive thus for current calculation, the following jamming angle is assumed:

$$\rho_{\mathrm{f}}(H) = \arcsin\left(\frac{H - \frac{b}{a}t}{b_w}\right) \tag{1.27}$$

The proposed jamming angle could affect the moment characteristic of shallow sections during the second half when it turns out to result in just a small moment increase. In the estimation of the energy absorbed, the increased moment can be neglected. The value of H and r are obtained by minimizing the mean crushing moment M_m, so the following limitation can be considered:

$$\frac{\mathrm{d}M_m(H,r)}{\mathrm{d}H} = \frac{\mathrm{d}M_m(H,r)}{\mathrm{d}r} = 0 \tag{1.28}$$

Equation (1.28) results in two equations and two unknown parameters which are H and r. Both are calculated to show half of the folding wavelength and small radius of the toroidal surface respectively. Substituting H and r into (1.25) to obtain the instantaneous moment expressed in terms of the rotation angle θ:

$$M = M_m \tag{1.29}$$

This derivation work of the plastic collapse is an approximation which can be applied when H and r do not change during the collapse of the section. In the present study, numerical technique was employed to solve the implicit, nonlinear equations using MATLAB™.

5. Development of Finite Element Model

5.1. Model Geometry, Material Model, and Finite Element Mesh

The three procedures follow those that have been adopted by the author in the previous work [13]. The hat-section tube is composed of a hat-section and a closed-plate. Strength is important with regard to hat-section, as they are often produced to support heavy loads and resist bending. Generally, both parts are spot-welded together to form a section that is symmetrical with respect to the y axis as shown in Fig. 4. In the previous work [13], bolted connections were used to secure both parts either during or after the test. Robust shell elements type S4R were assigned to model the tubes which is a four-noded quadrilateral element with six degrees-of-freedom (dof) per node. The tubes were partitioned into half model due to symmetry.

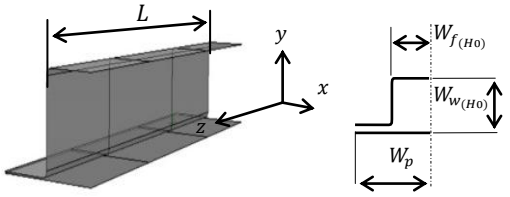

Fig. 4: Half model geometry of hat-section tubes

Table 1: Design dimensions of hat-section tube (Unit: mm)

Part	Web	Flange	Lip	Width	Length	Thickness
Hat-section	30	60	30	-	-	1
Closed-plate	-	-	-	120	300	1

5.2. Mesh Convergence, Connectors, and Boundary Condition

In the previous study, during validation of the FE model, the preliminary simulation of the tubes showed that the crush force converges as the mesh density increases. This indicates that the chosen element size for each region of the tube is appropriate. In the case of pure bending, the section of first fold was modelled with finer mesh (2 x 2 mm^2) as shown in Fig. 5. The bolted connections were modelled as mesh-independent spot welds which are rigid models. All boundary conditions were assigned according to the previous work [11].

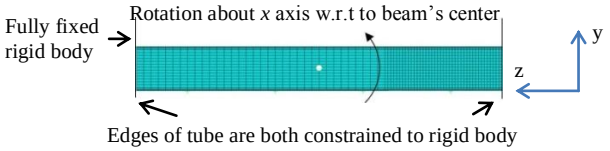

Fig. 5: A FE mesh of the half model subject to pure bending

6. Validation Results of the Modified Theoretical Model

The primary output of the modified mathematical model is the moment-rotation relationship. In order to validate the accuracy, several simulations were performed. The quantitative analysis in the validation procedure involves the comparison of the moment-rotation characteristics of the simulation and the calculated mathematical model. Effective simulation of bending behaviour of the FE model would capture the global and buckling collapse behaviour of the hat-section tubes. Several iterations were simulated by using different dimensional parameters.

Table 3: Sections dimension and measured values

Section	Dimension (mm)			W_f/t	W_f/W_w	H (mm)	r (mm)
	W_f	W_w	W_l				
S1	60	30	30	60	2.00	20.00	20
S2	60	30	20	60	2.00	20.00	20
S3	100	30	30	100	3.33	40.00	140
S4	30	50	30	30	0.60	55.00	22

6.1. MATLAB Programming

For solving Equation (1.28), MATLAB for numerical computation was used and a program for the calculation was developed. The input data for MATLAB program is listed in Table 4.

Table 4: MATLAB input measurements

Input	Symbols		Input	Symbols
Yiels stress	σ_y		Web width	W_w
Segment rotation	θ		Lip	W_l
Half rotation	ρ		Radius of curvature	r
Plastic bending moment	m_p		Shell thickness	t
Flange width	W_f		Half hinge length	h

6.1. Validation Results for Hat-Section Tubes under Pure Bending

The modified theoretical models for purely bent hat-section tubes produced good agreement against simulation results as shown in Fig. 6 and 7. The calculated moment carrying capacity in both graphs show dramatic decrease as the plastic hinge rotation angle increases. Both calculated values were exponentially raised up because the onsets of collapse of these beams were not defined in the model in order to reduce the complexity of the formulation. The onsets of collapse should have occurred at the point of maximum moment but not from the origin as the FE simulation results. Kecman [3] in his model had predicted this point in a quite accurate prediction. Nevertheless, the modified analytical model and simulation results are still matched up well and the calculation managed to give adequate predictions for the former than the latter. In the first 10° of rotation, the modified theory seems to underestimate the load capacity of simulation result as shown in Fig. 6. The discrepancy however less than 10% and this could possibly happen due to extensive strain hardening during initial folding exhibited by simulation trend. The proposed analytical predictions showed good agreement with simulation.

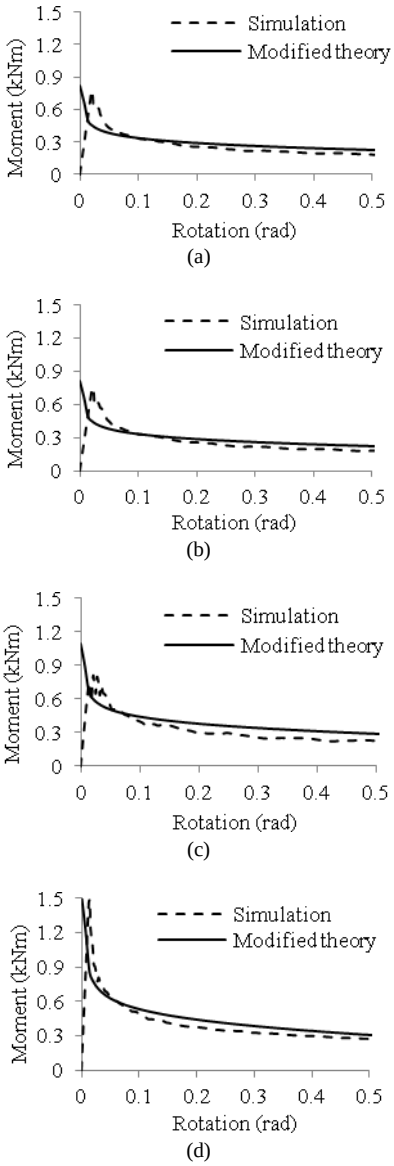

Fig. 6: A Moment-rotation relationship: (a) S1, (b) S2, (c) S3 and (d) S4 (simulation vs. modified theory)

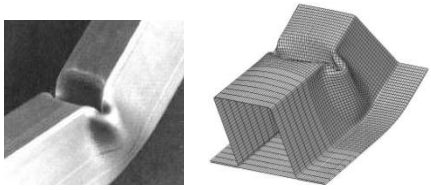

(a) (b)

Fig. 7: A (a) Kecman collapse model and (b) present simulation (S4)

7. Conclusion

Theoritical collapse models of square and rectangular tubes were modified to predict the collapse mechanism and moment-rotation

relationship of steel hat-section tubes. The modified theoretical model provides an adequate accuracy on qualitative and quantitative estimation of the moment variation. They were compared with simulation of pure bending of the tubes at different cross section. This indicates the effectiveness of kinematic method in modelling the rigid, perfectly plastic bending collapse of hat-section tubes. Even though the modified theory was initially developed for axial loading analysis, it applies well with bending problem of thin-walled tubes. In the present study, the calculation procedure is common for all type of hat-section tubes made of ductile materials. The modified analytical approach is considered kinematically admissible when the stretching deformation at the corner area that creates the toroidal region is included.

Acknowledgment

The authors gratefully acknowledge the help of the Universiti Teknologi MARA (UiTM) and IRMI of UiTM in providing the Lestari Fund research grant (600-IRMI/MyRA 5/3/LESTARI (023/2017)).

References

[1] I. Kallina, F. Zeidler, K. Baumann, and D. Scheunert, "The offset crash against a deformable barrier, a more realistic frontal impact," in *Proceedings: International Technical Conference on the Enhanced Safety of Vehicles*, 1995, pp. 1300-1304.

[2] T. Wierzbicki and W. Abramowicz, "On the crushing mechanics of thin-walled structures," *Journal of Applied mechanics*, vol. 50, pp. 727-734, 1983.

[3] D. Kecman, "Bending collapse of rectangular and square section tubes," *Int J Mech Sci*, vol. 25, pp. 623-636, 1983.

[4] T. Wierzbicki, L. Recke, W. Abramowicz, T. Gholami, and J. Huang, "Stress profiles in thin-walled prismatic columns subjected to crush loading-II. Bending," *Computers & structures*, vol. 51, pp. 625-641, 1994.

[5] T. Kim and S. Reid, "Bending collapse of thin-walled rectangular section columns," *Comput Struct*, vol. 79, pp. 1897-1911, 2001.

[6] W. Chen, "Experimental and numerical study on bending collapse of aluminum foam-filled hat profiles," *Int J Solids Struct*, vol. 38, pp. 7919-7944, 2001.

[7] G. Belingardi and A. Scattina, "Experimental investigation on the bending behaviour of hybrid and steel thin walled box beams—The role of adhesive joints," *Int J Adhes Adhes*, vol. 40, pp. 31-37, 2013.

[8] K. Sato, T. Inazumi, A. Yoshitake, and S.-D. Liu, "Effect of material properties of advanced high strength steels on bending crash performance of hat-shaped structure," *Int J Impact Eng*, vol. 54, pp. 1-10, 2013.

[9] H. Hashim, A. R. Ab Ghani, and W. Kuntjoro, "Bending Response and Energy Absorption of Closed-Hat-section Beams," *Modern Applied Science*, vol. 10, p. 225, 2016.

[10] H. Zhang, G. Sun, Z. Xiao, G. Li, and Q. Li, "Bending characteristics of top-hat structures through tailor rolled blank (TRB) process," *Thin-Walled Structures*, vol. 123, pp. 420-440, 2018.

[11] H. Hashim, A. R. A. Ghani, and W. Kuntjoro, "Bending Collapse of Closed-hat-section Beams. Part II: Theoretical Model Modification and Validation," *Journal of Mechanical Engineering*, pp. 57-69, 2017.

[12] H. Mahmood, A. Paluszny, and Y. Lin, "Bending deep collapse of automotive type components," SAE Technical Paper 0148-7191, 1988.

[13] H. Hashim, A. R. A. Ghani, and W. Kuntjoro, "Bending Collapse of Closed-hat-section Beams. Part I: Development and Validation of Finite Element Models," *Journal of Mechanical Engineering*, pp. 57-69, 2017.